DESIGN OF DIGITAL PHASE-LOCKED LOOPS FOR ADVANCED DIGITAL TRANSPONDERS

Tien M. Nguyen, IEEE Senior Member, Hen-Geul Yeh, IEEE Senior Member
Sami M. Hinedi, IEEE Member, Charlie Kyriacou, IEEE Member

Jet Propulsion Laboratory
California Institute of Technology
4800 Oak Grove Drive
Pasadena, CA 91109

Abstract

For advanced digital space transponders, the Digital Phased-Locked Loops (DPLLs) can be designed using the available analog loops. DPLLs considered in this paper are derived from the Analog Phase-Locked Loop (APLL) using S-domain to Z-domain mapping techniques. Three mappings are used to develop digital approximations of the APLL, namely, Bilinear Transformation (BT), Impulse Invariant Transformation (IIT) and Step Invariant Transformation (S11) techniques. Numerical results using typical parameters employed by NASA's standard transponder are presented as an example. The performance in terms of the closed loop phase and magnitude responses, carrier tracking jitter, and response of the loop to the phase offset (between the incoming phase and reference phase) are evaluated for each digital approximation. theoretical results of the carrier tracking jitter for signal with data modulation-on and signal with data modulation-off cases are then validated by computer simulation. Both 'theoretical and computer simulation results show that at high sampling frequency, the DPLL approximated by all three transformations have the same tracking jitter. However at low sampling frequency, the digital approximation using BT outperforms the others. Minimum sampling frequency for adequate tracking performance is determined for each digital approximation of the analog loop. In addition, computer simulation shows that the DPLL developed by BT provides faster response to the phase offset than IIT and SIT.

1. introduction

Migration towards a full digital-implementation of the space transponders is currently one of the main objectives in satellite/spacecraft transponders design. The use of DPLL is increasingly becoming popular for both satellite and spacecraft transponder applications. In recent years, the topic of DPLL has been studied in great detail and well documented in the literature [1 - 11]. Reference [1] provided excellent survey of the work accomplished during 1960- 19S0. References [4-6] dealt with the analysis, design and performance of the DPLL. References [7-8] discussed optimum DPLL and digital approximation of the analog loop filter. References [1 0-11] presented various algorithms for implementing the DPLL. Currently, most of the work on DPLL concentrates in these areas, and very little on the optimum digital approximation of the APLL [8-9]. Reference [8] dealt only with the design of an optimum loop filter using IIT, minimization method, estimation-prediction technique, and classical control theory approach. The digital loop filters derived by these methods were compared in [8] in terms of stability, gain margin, steady state and transient performance. On the other hand, [9] focused on the design of the DPLL based on the APLL. Reference [9] considered four different transformations, namely, Bilinear Transformation (BT), Impulse Invariant Transformation (IIT), Step Invariant Transformation (SIT) and Rotational Transformation (RT). The output phase responses of the approximated digital loops using these transformations, for low sampling rates, were evaluated in the absence of noise and compared. It was found in [9] that for a simple second order APLL, the phase response of the digital approximation of the APLL using I IT method exhibits less overshoot and ringing than the others.

The present work is an extension of [8, 9 and 14] to include many other aspects in determining an optimum transformation technique to develop a good digital approximation of a given APLL. The digital approximation is developed by mapping the continuous time S-domain to the discrete time Z-domain. The mapping is accomplished using BT, IIT, SIT, and RT. Because the RT is identical to IIT technique, only three techniques, namely, BT, IIT and SIT are considered in this paper. For each of these mapping techniques, the phase and magnitude responses of the closed-loop transfer function, the response of the loop to the phase offset, the minimum sampling frequency for adequate tracking performance; and the carrier tracking jitter will be evaluated.

The paper is divided into 5 sections. Section 2 introduces the typical earth-to-space (or the uplink)

signal format to be received by the analog space transponder along with a simplified model of the typical APLL for tracking the uplink carrier. Note that the uplink signal can have either command data modulation on or off. Equivalent DPLL's are also described in this section. Detailed recursive implementations of the DPLL's using BT, IIT and SIT are described in Section 3. Included in Section 3 are the plots of the phase and magnitude responses of the closed-loop transfer functions for each digital approximation of the APLL using the NASA's standard transponder as an example. Section 4 derives the carrier tracking phase jitter for both analog and digital loops with the command modulation-on and command modulation-off. Section 5 presents the computer simulation results to verify the theoretical results obtained in Section 4 and to determine the transient response of the digital loops to the initial phase offset. Furthermore, computer simulation results for determining the minimum sampling frequency for each approximation are also presented in Section 5. Section 6 presents the key conclusions of the paper.

2. System Modeling

The mathematical model for the typical uplink signal, from the ground station to the spacecraft transponder, $S(t)$, is defined as:

$$S(t) = \sqrt{2P}\sin(\omega_C + \omega_d)t + \Theta(t) + \varphi) \tag{1}$$

where P denotes the total received power, $\omega_C = f_C$ is the angular uplink carrier frequency, ω_d is Doppler angular frequency offset, $\Theta(t)$ characterizes the phase modulation, and φ characterizes the phase offset. The phase modulation employed by the typical space transponder is: $\Theta(t) = md(t)\sin(\omega_{SC}t) + m_R R(t)$, where m is the uplink command data modulation index, d(t) denotes the uplink Non-Return-to-Zero (NRZ) data, $\omega_{SC} = 2\pi f_{SC}$ is the uplink angular subcarrier frequency, m_R is the ranging modulation index, and $R(t)$ denotes the ranging signal,

Without loss of generality, one can set $\omega_c = 2\pi f_{IF}, \omega_d = 0, \varphi = 0$, and expand Eqn (1) to get

$$S(t) = \sqrt{2P}[\cos((3(t))\sin(2\pi f_{IF}t) + \sin(\Theta(t))\cos(2\pi f_{IF}t)] \tag{2}$$

Ignoring the higher order harmonic component, it can be shown that the first term in Eqn (2) represents the uplink carrier component, and the second is the uplink data component [16]. Presently, the

carrier component is tracked by an APLL. Illustrated in Figure 1 is a simplified block diagram of a typical analog carrier tracking loop which is currently employed by the NASA's standard space transponder. For typical NASA standard space transponder, the APLL depicted in Figure 1 is second order loop with the following characteristics:

$$\text{-Ib'} = Loop\,Gain = 2.4 \times 10^{7} \tag{3}$$

$$B(S) = \frac{1}{(1 + \tau_{RC}S)}, \quad \tau_{RC} = 1.6\times10^{-5}\,\text{sec} \tag{4}$$

$$F(S) = \frac{1 + \tau_2 S}{1 + \tau_1 S}, \quad = \quad 4707 \quad \text{sec}, \quad \tau_1 = 0.0442\,\text{sec} \tag{5}$$

$$V(S) = \frac{1}{(1 + \tau_V S)}, \quad \tau_V \quad 1.0\times10^{-6}\,\text{sec} \tag{6}$$

$$K(s) = \frac{1}{S} \tag{7}$$

Note that $B(S)$ is the typical Low-Pass Filter (LPF), $F(S)$ is the loop filter, $V(S)$ is the roll-off filter of the VCO, and $K(S)$ is the VCO integrator. Let $G(S)$ be the transfer function (excluding the ideal integrator $K(S)$) of the analog loop defined as follow:

$$G(s) = B(S)F(S)V(s) \tag{8}$$

Based on the APLL described in Figure 1, the equivalent digital counterparts are shown in Figures 2 and 3. Figure 2 shows the first configuration, the so called Configuration I, for the digital approximation of the analog loop. Configuration I is developed using direct transformation of each functional block in the analog loop (i.e., $B(S), F(S), V(S)$ and $K(S)$) into the Z-domain. On the other hand, Configuration II shown in Figure 3 is developed by transforming, the composite function $G(S)$ and $K(S)$ into the Z-domain, respectively. Notice that the digital approximations of the APLL illustrated in Figures 2 and 3 have the sum-and-dump circuit to reduce the sample rate by a factor of M before digital filtering. The sample rate is reduced to a rate such that the implementation of the digital filter is feasible using current digital signal processors. In the following section, the recursive implementations of the LPF, VCO roll-off filter, loop filter, VCO integrator, and the transfer function $G(S)$ will be described,

3. Recursive Implementations B(S), F(S), V(S), G(S) and K(S)

To obtain the digital approximation of the analog carrier PLL described in Figures 2 and 3 each functional block in the analog loop (i e., $B(S), F(S), V(S)$ and $K(S)$) can be mapped direct] y into the Z-domain using BT and the composite function $G(S)$ using IIT or SIT, respectively. Notice that when using the BT technique, one does not map the composite function $G(S)$ because of its mathematical complexity associated with this technique. Moreover, when using the I IT and SIT techniques, ones does not map each functional block in the analog loop because one wants to preserve the impulse and and step responses of the loop, respectively, at the sampling points. Therefore, this section will deal only with BT/IIT/SIT, and that BT and IIT/SIT correspond to Configuration I and II, respectively.

3.1. Bilinear Transformation Method

With proper sampling frequency, this method preserves the phase characteristics in the narrow pass-band when mapping the analog PLL into the digital domain. The mapping from analog (S-domain) to discrete domain (Z-domain) can be achieved by direct substitution of the following equation into the analog transfer function [12- 14]

$$S = \frac{2\ (z-1)}{T_S\ (Z+1)} \tag{9}$$

where T_S denotes the sampling period, and $F_S = 1/T_S$ denotes the sampling frequency. To obtain the digital approximation of the analog filters using bilinear transformation, one substitutes Eqn (9) into Eqns (4), (5), (6) and (7) to get $B(Z)$, loop filter $F(Z), V(Z)$ and $K(Z)$. The results are,

$$B(z) = \frac{(1+Z^{-1})}{(A_{00}+A_{11})} \tag{10}$$

$$F(Z) = \frac{(A_0 Z - B_0)}{(A_1 Z - B_1)} \tag{11}$$

$$K(z) = \frac{T_S\ (Z+1)}{2\ (Z-1)} \tag{12}$$

where

$$A_{00} = 1 - C_0,\ A_{11} = 1 + C_0, \tag{13}$$

$$A_0 = 1 + a_0, A_1 = 1 + b_0,\ B_0 = a_0 - 1,\quad B_1 = b_0 - 1 > 0 \tag{14}$$

and

$$C_0 = \frac{2\tau_{RC}}{T_S}, \quad a_0 = \frac{2\tau_2}{T_S}, \quad b_0 = \frac{2\tau_1}{T_S} \tag{15}$$

Note that the Z-domain representation for $V(S)$ is exactl y the same as Eqn (1 O) except that C_0, A_{oo} and Al_1 are replaced by, respectively

$$C_{01} = \frac{2\tau_V}{T_S}; \quad .4_1 = 1 - c_0; \quad .4_{oo} = 1 + C_{01} \tag{16}$$

The digital closed-loop transfer function, $H(Z)$, for this case is given by

$$H(Z) = \frac{AK \cdot B(Z)F(Z)V(Z)K(Z)}{[1 + AK \cdot B(Z)F(Z)V(Z)K(Z)]} \tag{17}$$

Using the typical values for NASA's standard transponder, plots of the analog and digital closed-loop phase and magnitude responses are shown in Figures 4a and 4b. These figures show that for sampling frequencies below 80 KHz, distortions in phase and magnitude can occur for the digital approximation loop. In addition, the figures show that for sampling frequencies greater than or equal to 80 KHz the response of the digital loop approaches that of the analog counterpart. Hence, to achieve the same response as the analog loop, the minimum sampling frequency for this case is 80 KHz. Later on, the minimum sampling frequency to achieve acceptable tracking performances will be investigated by computer simulation. Figures 5a, 5b and 5c depict the recursive implementation of the loop filter $F(Z)$, the integrator $K(Z)$ and the LPF $B(Z)$, respective] y.

3.2, impulse Invariant Transformation Method

This mapping technique preserves the impulse response at the sampling points. Let $g(t)$ be the impulse response of $G(S)$, i e., $g(t) = L^{-1}$ [G(S)}, where $L^{-1}\{.\}$ denotes the inverse Laplace transform of {.}, Thus, the digital approximation of the analog transfer function $G(S)$ is given by [12-14]

$$G_D(Z) = T_S \cdot z\{g(t)|_{t=nT_S}\} \tag{18}$$

where z{. } is the z-transform of {.}. Note that the analog transfer function $G(S)$ considered in this

paper is defined as in Eqn (8). Using Eqn (18), one can find the relationship between the S-variable and Z-variable; it is given by [12-14]

$$S = \frac{(Z-1)}{T_S Z} \tag{19}$$

To obtain the equivalent digital approximation for the integrator $K(S)$, one substitutes Eqn (19) into Eqn (7) to get

$$K(Z) = \frac{ZT_S}{(Z-1)} \tag{20}$$

The digital approximation for the analog transfer function $G(S)$ (see Eqn (8)) is obtained by finding the inverse Laplace transform of $G(S)$ and then substituting the resultant into Eqn (18). Evaluating Eqn (1 *8), one* has

$$G_D(Z) = T_S \left[\frac{\alpha_0}{1 - Z^{-1} e^{aT}} + \frac{\alpha_1}{1 - Z^{-1} e^{bT}} + \frac{\alpha_2}{1 - Z^{-1} e^{cT}} \right] \tag{21}$$

where

$$a. = \frac{\tau_1 - \tau_2}{(\tau_1 - \tau_{RC})\ (\tau_1 - \tau_{1'})} \tag{22}$$

$$\alpha_1 = \frac{\tau_{RC} - \tau_2}{(\tau_{RC} - \tau_1) \cdot (\tau_{RC} - \tau_{1'})} \tag{23}$$

$$\alpha_2 = \frac{\tau_{1'} - \tau_2}{(\tau_2 - \tau_1)\ (\tau_{1'} - \tau_{RC})} \tag{24}$$

and

$$a = \frac{1}{\tau_1},\ b = \frac{1}{\tau_{RC}},\ c = \frac{1}{\tau_{1'}} \tag{25}$$

The digital closed-loop transfer function for this case is given by

$$H(Z) = \frac{AK \cdot G_D(Z) K(Z)}{[1 + AK \cdot G_D(Z) K(Z)]} \tag{26}$$

From Eqn (26), the plots of the phase and magnitude responses can be obtained for the digital approximation loop. Figures 6a and 6b illustrate the closed-loop phase and magnitude responses for both analog and digital loops using typical parameters employed by NASA's standard transponder.

The figures show that the response of the digital loop approximated using impulse invariant transformation is the same as analog loop when the sampling frequency is higher than or equal to 80 KHz, When sampling frequency is less than 80 KHz, the digital loop can encounter serious distortion in both phase and amplitude responses. The recursive implementations $G_D(Z)$ and $K(Z)$ using impulse invariant transformation are shown in Figures 7a and 7b, respectively.

3.3 Step Invariant Transformation Method

This method preserves the step response at the sampling points when mapping S-domain to Z-domain. Similar to Section 3.2, the relationship between the analog and digital transfer function is [12-14]

$$G_D(Z) = \frac{Z-1}{Z} \cdot z\left\{ \left[L^{-1}\left[\frac{G(S)}{S}\right] \right]_{t=nT_s} \right\} \tag{27}$$

where $z\{.\}$ and $G(S)$ are defined the same as above. Using Eqn(27), one also can determine the relationship between S and Z-variable. It is found to be [12-14],

$$S = \frac{(Z-1)}{T_S} \tag{28}$$

Digital approximations $K(Z)$ and $G_D(Z)$ for $K(S)$ and $G(S)$ using step invariant transformation can be obtained by using Eqns (27) and (28). The results are:

$$K(z) = \frac{T_S}{(Z-1)} \tag{29}$$

$$G_D(Z) = \beta_0 + \beta_1 \cdot \left[\frac{1-Z^{-1}}{1-Z^{-1}e^{-aT_S}}\right] + \beta_2 \cdot \left[\frac{1-Z^{-1}}{1-Z^{-1}e^{-bT_S}}\right] + \beta_3 \cdot \left[\frac{1-Z^{-1}}{1-Z^{-1}e^{-cT_S}}\right] \tag{30}$$

where

$$\beta_0 = \frac{\alpha_0}{a} + \frac{\alpha_1}{b} + \frac{\alpha_2}{c} \tag{31}$$

$$P, = -\frac{\alpha_0}{a}, \beta_2 = -\frac{\alpha_1}{b}, \beta_3 = -\frac{\alpha_2}{c} \tag{32}$$

The parameters $\alpha_0, \alpha_1, \alpha_2$, a, b, and c are defined in Eqns (22)-(25), respectively. Again, Eqn (26) can

be used to evaluate the closed-loop transfer function for this case. Using typical values employed by NASA's standard transponder, plots of the closed-loop transfer functions for both analog and digital loops are shown in Figures 8a and 8b. The figures show that the magnitude response approaches the analog response when the sampling frequency is higher than or equal to 100 KHz. However, the phase response suffers serious distortion when the sampling frequency is less than 1 MHz. Thus, in order to achieve the same response as the analog loop, the digital approximation loop using step invariant transformation must be sampled at least at 1 MHz, i e., this method requires 10 times higher sampling frequency than the previous methods. Table 1 summarizes the results for the minimum sampling frequency, F_S, that is required for the digital loop to achieve the same phase and amplitude responses using typical parameters of the NASA's standard transponder. The recursive implementations of $G_D(Z)$ and $K(Z)$ using step invariant transformation are shown in Figures 9a and 9b.

Table 1: Minimum Sampling **Frequency,** F_S, Required for the Digital Approximation to Achieve the Same Phase and Amplitude Responses as **APLL** Using Typical Parameters for NASA's Standard Transponder

Transformation Method	Minimum F_S Required to Achieve the Same Analog Phase and Amplitude Responses, KHz
Bilinear	80
Impulse Invariant	880
Step Invariant	10000

4. **Carrier** Tracking **Performances** of (he Approximated Digital **Loops**

The tracking performance of the APLL for high loop Signal-to-Noise Ratio (LSNR) is well-known [1 5-16]. For LSNR > 5 dB, the variance of the tracking phase error is approximated by

$$\sigma_\Phi^2 = \frac{N_0 B_L}{P_C} \tag{33}$$

where N_0 is the one-sided thermal noise spectral density, B_L denotes one-sided tracking loop noise bandwidth, and P_C is the carrier power. Note that LSNR = 5 dB is the loop threshold point where the nonlinear theory and linear theory departs severely (by about 1 dB or more in terms of tracking vari-

ante). The mathematical expressions for the analog loop bandwidth is given by [15-16]

$$B_L = \frac{1}{2\pi}\int_{-\infty}^{\infty}|H(j\omega)|^2 d\omega \tag{34}$$

where $H(j\omega)$ is the analog closed loop transfer function which is identical to Eqn (17) with Z replaced bys $= j\omega$. Using the loop gain, the LPF, the loop filter, the roll-off filter of the VCO, and the VCO integrator given in Eqns (3)-(7), respectively, the one-sided tracking loop noise bandwidth is calculated using Eqn (34) resulting in $B_L = 62$ Hz.

For the digital loops, the one-sided loop noise bandwidth B_{DL} is given by

$$B_{DL} = \frac{1}{4\pi j T_S J^2(1)}\oint_{|Z|=1} H(Z)H(Z^{-1})\frac{dZ}{Z} \tag{35}$$

where $j = \sqrt{-1}$, and $H(Z)$ is the closed loop digital transfer function which is given by Eqn (17) and (26) for BT and IIT/SIT respectively. The digital loop noise bandwidth for IIT can be calculated by substituting the digital transfer function $G_D(Z)$, shown in Eqn (21), into Eqn (26) and then substituting the resultant into Eqn (35). Similarly, for SIT, Eqn (28) is used instead of Eqn (21) for the digital transfer function $G_D(Z)$.

In this paper, Eqn (35) will be evaluated numerically using an analytical computer program for three transformation methods under investigation. The numerical results are plotted in Figure 10 using typical values for NASA's standard transponder. Figure 10 shows a plot B_L/F_S (or $B_L T_S$) vs B_{DL}/F_S (or $B_{DL}T_S$) for BT, IIT and S1'1'. This figure shows that, for $B_L T_S \leq 0.01$, the tracking loop noise bandwidth of the digital approximation of the analog loop using BT is almost identical to the analog loop. On the other hand, the digital loop noise bandwidth obtained by using IIT/SIT departs from the analog loop bandwidth when $B_L T_S \geq 0.001$. Notice that SIT provides the worst digital approximation, and BT is the best among the three transformations. Table 2 gives a brief summary of the numerical

results shown in Figure 10.

Table 2: Loop Noise Bandwidth of the Digital Approximations of the Analog PLL Using Typical Values for NASA's Standard Transponder When F_S = 6.2 **KHz** and 62 KHz

Transformation Method	Analog Loop Noise Bandwidth, B_L	Digital Loop Noise Bandwidth, B_{DL}, at F_S = 6.2 KHz	Digital Loop Noise Bandwidth, B_{DL}, at F_S 62 KHz
Bilinear	62 Hz	62 Hz	62 Hz
impulse Invariant	62 Hz	76.88 Hz	62 Hz
Step Invariant	62 Hz	114.08 Hz	62 Hz

Figure 10 shows that, for $B_L T_S \leq 0.01$ (corresponding to $F_S \leq 6.2$ KHz), the digital tracking loop bandwidth approximated by BT is the same as the analog loop. Moreover, the loop bandwidth of the digital loops approximated by IIT and SIT are worst than that of the analog counterpart for $B_L T_S \geq$ 0.001 (corresponding to F_S = 62 KHz). This implies that in order to achieve the same tracking phase error as the analog loop, the digital loop approximated by the BT requires lower sampling frequency than IIT and SIT. For the analog loop with characteristics specified in Section 2, it is found that the minimum sampling frequency (for the digital loop) that is required to have the same tracking loop bandwidth as the analog is 6.2 KHz, and this is only achievable through BT. It has been shown in Section 3, Table 1, that the minimum sampling frequency required to achieve the same phase and amplitude responses as the analog is 80 KHz for both BT and 11-1', and 1 MHz for SIT. Hence, what will be the minimum sampling frequency that one would select for optimum performance ? The answer to. this question will be deferred until Section 5.

It should be mentioned that Eqn (35) can also be evaluated analytically by expressing $H(Z)$ in the following form

$$H(Z) = \frac{b_0 Z^4 + b_1 Z^3 + b_2 Z^2 + b_3 Z^1 + b_4}{a_0 Z^4 + a_1 Z^3 + a_2 Z^2 + a_3 Z^1 + a_4} \tag{36}$$

and then from Table III in [17], Eqn (35) becomes

$$B_{DL} = \frac{1}{2T_S H^2(1)\, a_0 \{(a_0^2 - a_4^2) Q_0 - (a_0 a_1 - a_3 a_4) Q_1 + (a_0 a_2 - a_2 a_4) Q_2 - (a_0 a_3 - a_1 a_4) Q_3\}} \frac{a_0 B_0 Q_0 - a_0 B_1 Q_1 + a_0 B_2 Q_2 - a_0 B_3 Q_3 + B_4 Q_4}{} \tag{37}$$

where

$$B_0 = b_0^2 + b_1^2 + b_2^2 + b_3^2 + b_4^2; \quad B_1 = 2(b_0 b_1 + b_1 b_2 + b_2 b_3 + b_3 b_4) \tag{38}$$

$$B_2 = 2(b_0 b_2 + b_1 b_3 + b_2 b_4); \; B_3 = 2(b_0 b_3 + b_1 b_4); \; B_4 = 2 b_0 b_4 \tag{39}$$

$$Q_0 = a_0 e_1 e_4 - a_0 a_3 e_2 + a_4 (a_1 e_2 - e_3 e_4); \quad Q_1 = a_0 a_1 e_4 - a_0 a_2 a_3 + a_4 (a_1 a_2 - a_3 e_4) \tag{40}$$

$$Q_2 = a_0 a_1 e_2 - a_0 a_2 e_1 + a_4 (a_2 e_3 - a_3 e_2); \quad Q_3 = a_1 (a_1 e_2 - e_3 e_4) - a_2 (a_1 e_1 - a_3 e_3) + a_3 (e_1 e_4 - a_3 e_2) \tag{41}$$

$$Q_4 = a_0 \left[e_2 (a_1 a_4 - a_0 a_3) + e_5 (a_0^2 - a_4^2) - e_5^2 \right] [a_1 (a_1 - a_3) + (a_0 - a_4)(e_4 - a_2)] \tag{42}$$

$$e_1 = a_0 + a_2; \quad e_2 = a_1 + a_3; \quad e_3 = a_2 + a_4 \tag{43}$$

$$e_4 = a_0 + a_4; \quad e_5 = a_0 + a_2 + a_4 \tag{44}$$

As an example, for BT, one gets

$$a_0 = 2F_S A_{10} A_{11} + AKA_0; \; a_1 = 2F_S (A_{10} A_{00} + A_{01} A_{11} - A_{10} A_{11} B_1 - A_{11} A_{10} A_1) + AK(3A_0 - B_0) \tag{45}$$

$$a_2 = 2F_S A_1 (A_{00} A_{01} - A_{01} A_{11}) + 2F_S B_1 (A_{10} A_{11} - A_{10} A_{00} - A_{01} A_{11}) + 3AK(A_0 - B_0) \tag{46}$$

$$a_3 = 2F_S B_1 (A_{00} A_{10} - A_{01} A_{00} + A_{01} A_{11}) - 2F_S A_1 A_{01} A_{00} + AK(A_0 - 3B_0); \; a_4 = 2F_S B_1 A_{10} A_{00} - AKB_0 \tag{47}$$

$$b_0 = AKA_0; \quad b_1 = AK(3A_0 - B_0); \; b_2 = 3AK(A_0 - 3B_0) \tag{48}$$

$$b_3 = AK(3A_0 - B_0); \; b_4 = -AKB_0 \tag{49}$$

Having determined the corresponding digital loop noise bandwidth, one can evaluate the variance of the tracking phase error for the digital approximations of the analog loop using the following formula, from Eqn (33)

$$\sigma_\Phi^2 = \frac{NB_{DL}}{C} \tag{50}$$

where N is the total one-sided noise spectral density. When the uplink command data and ranging modulation are turned off, i.e., m $^{=}m_R$ = O, all power will be allocated to the carrier and there is no interference from the command data and ranging to the carrier tracking loop, and hence N = No. As the command data modulation (or ranging) is turned on, there exists some interferences between the carrier and the command data (or ranging). Since the ranging tones will be placed farther away from the carrier and the power allocated to the ranging is always smaller than the uplink command data, hence the effects of the ranging to the carrier tracking is negligible and will not be considered here. However, the interference effects of the uplink command data to the carrier tracking may not be neglected because of the increase in the uplink command data rate. Recently, the international Consultative Committee for Space Data Systems (CCSDS) has considered to increase the maximum uplink data rate from 2 Kbps to 4 Kbps and the possibility of using 32 KHz subcarrier frequency for both 2 Kbps and 4 Kbps.

To determine the effect of interference of the uplink data on the carrier tracking loop, a model of the uplink data must be provided. Here it is assumed that the uplink data symbols are equally likely to be +- I 's and -] 's and that successive symbol are uncorrelated. This assumption leads to the Power Spectral Density (PSD) of a unit power sinusoidal wave subcarrier phase-reversal-keyed by the uplink command data stream (see Eqn (1)) is given by [18]

$$S_{CD}(f, T, f_{SC}) = \sum_{n=2,\,n\,even}^{\infty} J_n^2(m)\,[\delta(f - nf_{SC}) + \delta(f + nf_{SC})] + \sum_{k=1,\,k\,odd}^{\infty} J_k^2(m)\,[S_D(f - kf_{SC}) + S_D(f + kf_{SC})] \tag{51}$$

where

$$S_D(f) = T\left[\frac{\sin(\pi fT)}{(\pi fT)}\right]^2 \tag{52}$$

where T is the command symbol period. Note that the PSD shown above is evaluated at the carrier frequency. Hence, when the command is on the total noise spectral density, N, seen by the carrier tracking loop can be evaluated using the following relationship

$$N = N_0\left[1 + \frac{P_C}{N_0} S_{CD}(B_{DL}, T, f_{SC})\right] \tag{53}$$

where P_c is defined as (from Eqn (1) and [16-18])

$$P_C = P \cdot (J_0(m))^2 \tag{54}$$

and $J_0(.)$ is the zero order Bessel Function. Using typical values for the NASA's standard transponder, Figure 11 shows the theoretical results obtained for the variance of the carrier tracking phase jitter, σ_ϕ^2, as a function of the received Signal-to-Noise spectral density Ratio (SNR), P/N_0, for both analog and digital loops when the command is on. The results were plotted for the modulation index $m = 70$ degree, uplink subcarrier frequency $f_{SC} = 32$ KHz, uplink command data rate R_S = 2 Kbps, and sampling frequency F_S = 1 MHz. As expected, for high sampling frequency the tracking jitter of the digital loop using BT/IIT/SIT approaches that of the analog loop. Figure 12 presents the numerical results for the digital loop using BT with both uplink command modulation-on anti off. The theoretical results shown in this figure will be verified by computer simulations in Section 5. Note that the relationship between the total received SNR, P/N_0, and the carrier tracking loop signal-to-thermal noise spectral density ratio, P_C/N_0 can be evaluated from Eqn (54), and the results are plotted in Figure 13.

s. Computer Simulation Rc.suits

The digital PLL's shown in Figures 2 and 3 have been implemented using the Signal Processing Workstation (SPW) of Comdisco, Inc. Simulations have been run to verify the carrier tracking jitter obtained in Section 4 and to determine the time responses of the digital loops due to the phase offset between the incoming and the NCO reference phase. The update rate of the loop has been set to be the same as the sampling rate. This is done in the simulation by setting the parameter M = 1 (see Figures 2 and 3). In addition, the simulations have been performed to determine the minimum achievable sampling frequency for each digital approximation.

S.1, Measurements of the Tracking Jitter and Time Response of the Digital Loops

Using typical parameters employed by the NASA's standard transponder, computer simulations for the digital loops approximated by BT (see Figure 2) and IIT/SIT (see Figure 3) have been run for both uplink command modulation-on (with modulation index set at 70 degree, uplink command data rate of 2 Ksps and subcarrier frequency of 32 KHz) and uplink command modulation-off at lMHz sampling frequency. The simulations were run for 2.5 million iterations, and the variance of the carrier phase jitter were measured for four different noise seeds and the average is presented in Table 3. For the

sake of comparison, the results are also plotted in Figure 12. On the other hand, Figure 14 shows the simulation results of the digital loops approximated by IIT and SIT at 1 MHz sampling frequency. The simulation results, for, all cases at 1 MHz sampling frequency, are in good agreement with the theoretical results.

Table 3: **Simulation** Results for **Command-On** With m = 70 Degree, ω_c = 32 KHz, R_S = 2 Ksps, and **Command-Off** at 1 **MHz** Sampling Frequency

P	Variance of The Carrier Phase Jitter, rad^2					
N0	Command - off			Command - on		
(dB-Hz)	BT	IIT	SIT	BT	IIT	SIT
30	0.064000	0.062250	0.063800	0.151000	0.150750	0.150250
35	0.019670	0.019175	0.019400	0.045100	0.044725	0.045250
40	0.006165	0,006013	0.006040	0.014000	0.013875	0.013875
45	0.001945	0.001895	0.001900	0.004398	0.004360	0.004355
50	0.000613	0.000598	0.000598	0.001390	0.001377	0.00137
55	0.000194	0.000189	0.000189	0.000441	0.000435	0.000445
60	6.145 x10-5	5.973 X10-5	5.960 x10-5	0.000139	0.000140	0.000140
65	1.955 x10-5	I .818X10-5	1 .890X 10-5	4.66x-10-5	4.623 x10-5	4,623 x10-5

Computer simulation has been performed to determine the time responses of the digital approximations of the analog loops using, the three transformation techniques described in Section 3. A phase offset of $\pi/9$ radian between the incoming phase of the signal and the reference NCO has been injected into the loop with 1 MHz sampling rate, and the settling time, t_S, of each loop to the phase offset was measured. Here, the settling time is defined as the time it takes the loop to catchup with the phase offset, or the time it takes the loop to stabilize in the presence of the phase offset. The results using typical parameters of NASA's standard transponder are summarized in Table 4 for command modulation-off and noise free case.

Table 4: Settling Time, t_S, for the phase offset of $\pi/9$ radians

Transformation Method	Settling Time, t_S, sec
Bilinear	0.12
impulse Invariant	0.14
Step Invariant	0.15

5.2. Minimum Achievable Sampling Frequency

As shown in Figure 10 and Table 2, for the analog PLL's characteristics specified in Section 2, the minimum sampling frequencies required for the digital loop to achieve the same analog tracking loop bandwidth are 6.2 KHz and 62 KHz for BT and for IIT/SIT, respectively. On the other hand, it has been shown in Section 3 that the minimum sampling frequencies required for the digital loop to have the same closed-loop phase and amplitude responses are 80 KHz and 1 MHz for BT/IIT and SIT, respectively. Based on these results, one is tempted to select the smallest sampling frequency so that the requirements on the speed of the digital signal processor and hence power consumption can be minimized, However, the selected, sampling frequencies (based on these criteria) may not be able to provide the required tracking performance. Computer simulation will be used as an additional tool to assist in the making of final decision on the minimum achievable sampling frequency. Here, the minimum achievable sampling frequency, denote as F_{Sm}, is defined as the frequency that satisfies the tracking performance requirement. Table 5 summarizes the simulation results for 200 KHz carrier frequency, 32 KHz subcarrier frequency, data rate of 2 Ksps, modulation index of 70 degree, P/N_0 of 35 dB-Hz and typical loop parameters employed by the NASA's standard transponder

Table S: Tracking Phase Jitter as a Function of Sampling Frequency for NASA's Standard Transponder

F_S, KHz	σ_ϕ^2, rad^2		
	BT	IIT	SIT
16.5	0.0725	Out-of-Lock	Out-of-Lock
18.5	0.0489	Out-of-Lock	Out-of-Lock
24.8	0.0476	Out-of-Lock	Out-of-Lock
240	0.0453	0.0458	Out-of-Lock
1000	0.0451	0.0447	0.0453

The phase jitters shown in Table 5 are then compared with the analog phase jitter of 0.045 rad^2 for this particular case (see Eqn *(50)* with B_{DL} replaced by $B_L = 621$ Hz). It is observed that the variance of the tracking phase error, σ_ϕ^2, of the digital loop approximated by BT is as good as the analog loop when the sampling frequency is about 24.8 KHz. Moreover, the tracking phase errors of the digital loops approximated by IIT and SIT are close to the analog loop when the sampling frequencies are 240 KHz and 1000 KHz, respectively. The results for the minimum achievable sampling frequency (or optimum sampling frequency) for the three transformations shown in Table 5 are then compared to the results obtained in Sections 3 and 4. Recall that Section 3 determines the minimum sampling frequency, denoted as F_{Smr}, that is required for the digital loops to achieve the same amplitude and phase responses as the analog loop, and Section 3 calculates the minimum sampling frequency, denote as F_{Smb}, for the digital loops to have the same tracking loop bandwidth as the analog loop. For typical NASA's standard transponder, Table 6 summarizes the final results regarding the optimum sampling frequency that is required for each digital approximation method. Table 6 shows that the minimum achievable sampling frequency for both BT and IIT is about four times F_{Smb} and, for SIT, the mini-

mum achievable sampling frequency is the same as F_{Smr}.

Table 6: **Minimum** Achievable Sampling Frequency for a Typical NASA's Standard Transponder

Transformation Method	Minimum Sampling Frequency Required to Achieve the Same Phase/ Amplitude Responses, F_{Smr}, KHz	Minimum Sampling Frequency Required to Achieve the Same Analog Loop Bandwidth, F_{Smb}, KHz	Minimum Achievable Sampling Frequency for a Specified Tracking Jitter, F_{Sm}, KHz	Remarks
BT	80	6.20	24.8	$F_{Sm} = 4F_{Smb}$
IIT	80	62,0	2400	$F_{Sm} = 3.9F_{Smb}$
SIT	1000	62.0	1000	$F_{Sm} = F_{Smr}$

6. Conclusion

Digital approximations of the analog carrier tracking loop for advanced digital transponder applications have been investigated in detail. Using Typical values of the loop parameters employed by the NASA's standard transponder, the performance of each approximation was determined for the closed loop phase and magnitude responses, carrier tracking jitter, response of the loop to the phase offset and minimum achievable sampling frequency. The numerical results show that BT appears to give the best performance at low sampling rate as compared to the other transformations. The best performance at low sampling frequency is evident from the closed loop phase and magnitude responses curves, carrier tracking loop bandwidths curves and the computer simulation results for the tracking phase error. However, at high sampling frequency (higher than or equal to 1 MHz, for the case considered in this paper), the performance of the DPLL approximated by all three transformations approaches that of the analog loop. It was found that in order to achieve the same tracking phase error as the analog loop, the minimum sampling frequencies required for BT/IIT and SIT are about $4F_{Smb}$ and F_{Smr}, respectively. Here, F_{Smb} and F_{Smr} denote the minimum sampling frequencies for the digital loops to have the same tracking loop bandwidth and phase/magnitude responses as the analog loop, respectively. In addition, using typical loop parameters for NASA's standard transponder, the simulation results show that the response to the incoming phase offset of $\pi/9$ radians of the digital loop approximated by the BT is faster than the loops approximated by IIT and SIT by about 20 and 30 msec, respectively

As pointed out in [9], in the absence of noise, the digital loop approximated by the IIT method

exhibits less overshoot and ringing in the output response than the others. However, this may not be the key criteria in the selection of the optimum transformation method for approximating the analog loop. This paper has shown that, for applications require low sampling frequency, the BT method appears to give the best performance in terms of the tracking phase error and response to the initial phase offset, Therefore,when the key requirements, such as low sampling rate, tracking phase error and fast response to the initial phase offset, for approximating the analog loop are desired then the BT method is recommended. Furthermore, the performance evaluation approach presented in this paper can easily be extended to any analog PLL to (1) find the minimum achievable sampling frequency, and (2) determine the tracking phase error of the digital approximation of the analog loop.

Acknowledgments

The authors thank S. Million and B. Shah for their assistance in computer simulation, R. Sadr and S. Kayalar for their useful comments and suggestions, and A. Kermode for his constant support. The research described in this paper was performed at the Jet Propulsion Laboratory, California Institute of Technology under Contract with National Aeronautics and Space Administration.

Reference

[1] William C. Lindsey, Chak M. Chic, "A Survey of Digital Phase-Locked Loops, " Proceedings of the IEEE, Vol. 69, No. 4, April 1981.

[2] Chak M. Chic, "Analysis of Digital Phase-1 ocked Loops," Ph.D. Thesis, University of Southern California, January 1977.

[3] J. K. Holmes, C. R. Tegnelia, " A Second Order All Digital Phase-I. ocked Loop," IEEE Transactions on Communication's, Vol. COM-22, January 1974.

[4] R. Sadr, W. J. Hurd, "Digital Carrier Demodulation for the DSN Advanced Receiver," TDA Progress Report 42-93, January-March 1988, Jet Propulsion Laboratory, Pasadena, CA.

[5] J. Garodnick, J. Greco, D. Schilling, "Response of All Digital Phase-Locked Loop," IEEE Transactions on Communications, Vol. COM-22, No. 6, June 1974.

[6] S. Aguirre, W. J. Hurd, "Design and Performance of Sampled Data Loops for Subcarrier and Carrier Tracking," TDA Progress Report 42-79, July-September 1984, Jet Propulsion Labora-

tory, Pasadena, CA.

[7] R. Kumar, W. J. Hurd, "A Class of Optimum Digital Phase-Locked Loops for the DSN Advanced Receiver," TDA Progress Report 42-83, July-September 1985, Jet Propulsion Laboratory, Pasadena, CA.

[8] S. Aguirre, W. J. Hurd, R. Kumar, J. Statman, "A Comparison of Methods for DPLL Loop Filter Design," TDA Progress Report 42-87, July-September 1986, Jet Propulsion Laboratory, Pasadena, CA.

[9] Dean J. Boman, "Performance of a Low Sampling Rate Digital Phase-Locked Loop," Master Thesis, Arizona State University, May 1987.

[10] C, R. Cahn, D. K. Leimer, "Digital Phase Sampling for Microcomputer implementation of Carrier Acquisition and Coherent Tracking," IEEE Transactions on Communications, Vol. Com-28, No. 8, August 1980.

[11 R. Cali, G. Ferrari, "Algorithms for Computing Phase and AGC in Digital PLL Receivers, " RF Design, October 1992.

[12] L. R. Rabiner, B. Gold, Theory and Applications of Digital Signal Processing, Englewood Cliffs, NJ: Prentice-Hall, 1975.

[13] W. D. Stanley, Digital Signal Processing, Reston, VA: Reston, 1975.

[14] Katshuiko Ogata, Discrete Signal Processing, Englewood Cliff, NJ: Prentice-Hall, 1987.

[15] Joe Yuen, Editor, Deep Space Telecommunications Systems Engineering, Chapters 3 and 5, Plenum Press, New York and London, 1983.

[16] Jack K. Holmes, Coherent Spread Spectrum Systems, Chapters 3 and 4, John Wiley & Sons, New York, 1982.

[17] E. I. Jury, Theory and Application of the z-Transform Method, Robert E. Krieger Publishing Company, Malabar, Florida, 1964.

[18] Tien M. Nguyen, "Closed Form Expressions for Computing the Occupied Bandwidth of PCM/PSK/PM Signals," IEEE/EMC-91 Proceedings on Electromagnetic Compatibility, New Jersey, Cherry Hills, August 1991.

Figure 1. Simplified Block Diagram of the Analog PLL

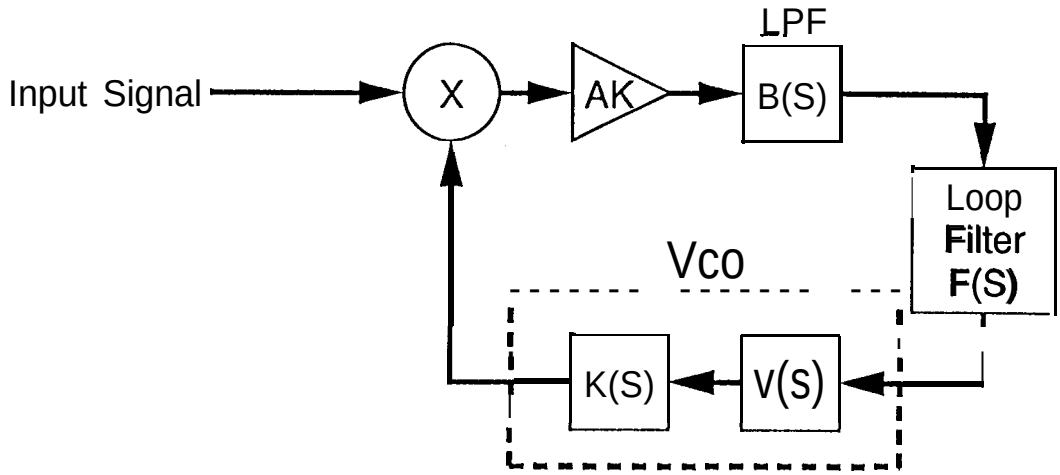

Figure 2. Digital Approximation of the Analog PLL – Configuration I

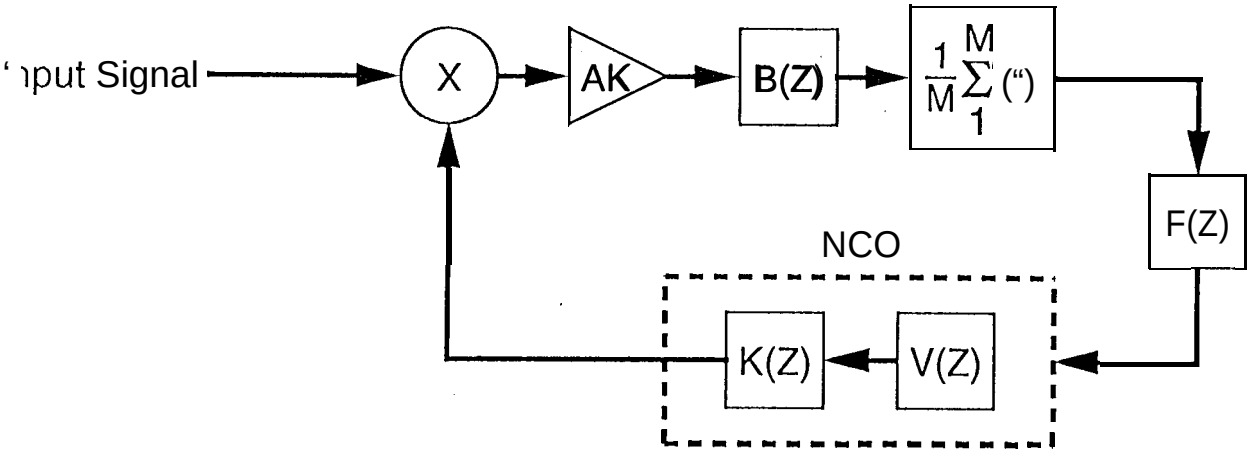

Figure 3. Digital Approximation of the Analog PLL – Configuration II

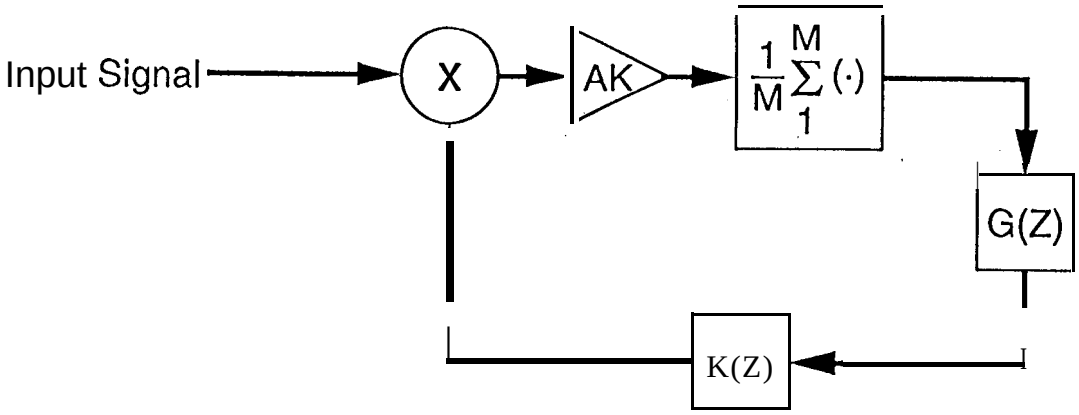

Figure 4. Closed-loop Response of the Digital Approximation Using Bilinear Transformation Method

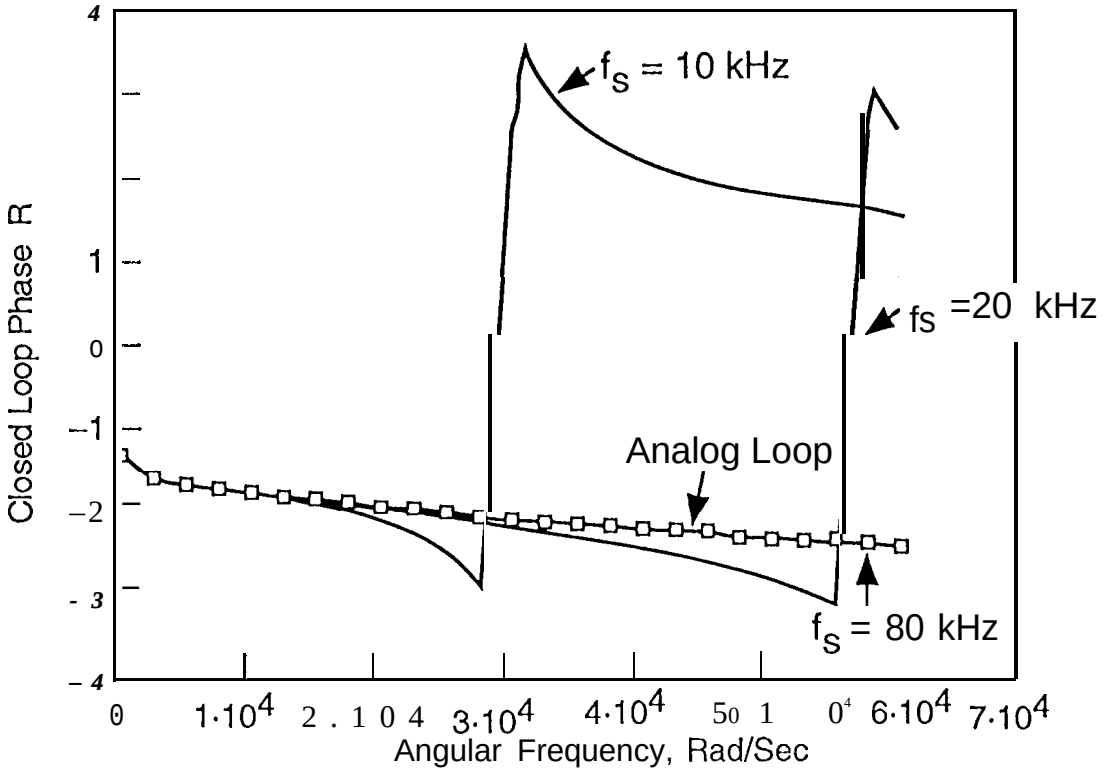

a. Plot of the Closed Loop Phase Characteristic

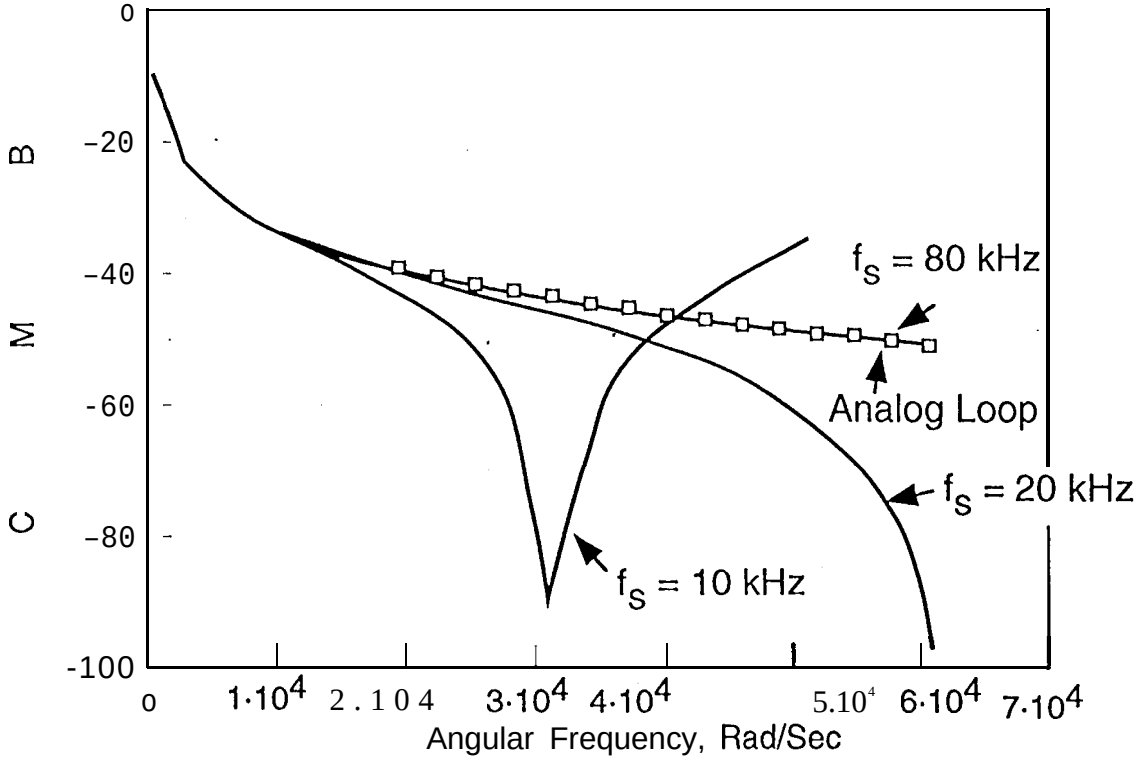

b. Plot of the Closed Loop Magnitude Response

Figure 5. Recursive Implementation of the Loop Filter, Lowpass and Filter and Integrator Using Bilinear Transformation

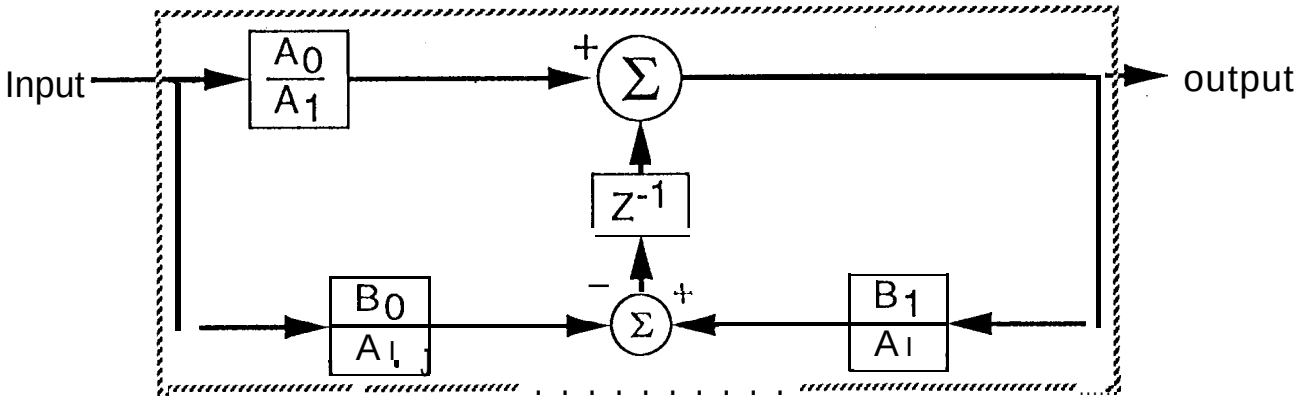

a. Loop Filter F(Z)

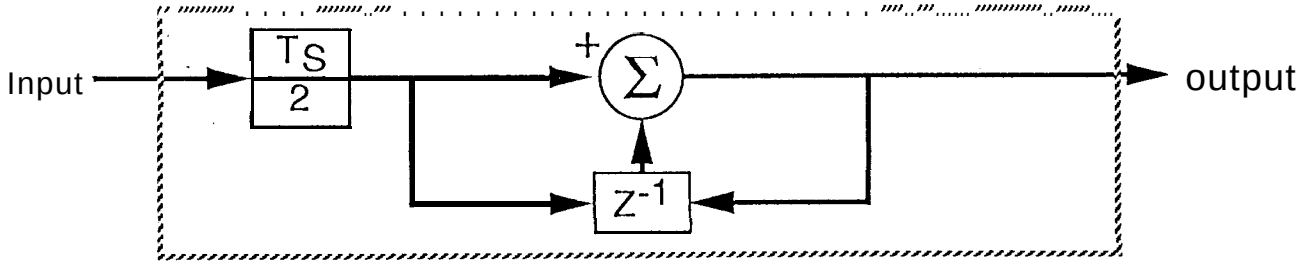

b. Integrator K(Z)

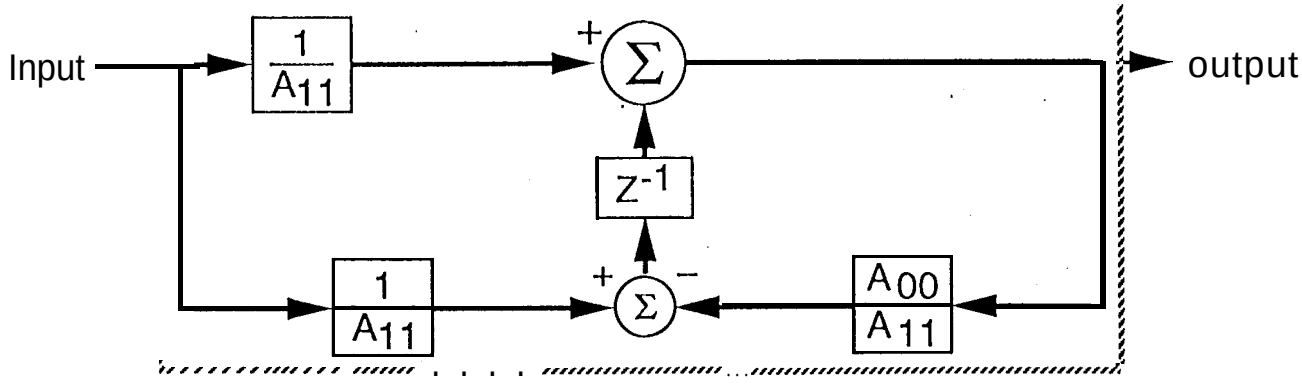

c. The Low Pass Filter B(Z)

Figure 6. Closed-loop Response of the Digital Approximation Using Impulse Invariant Transformation Method

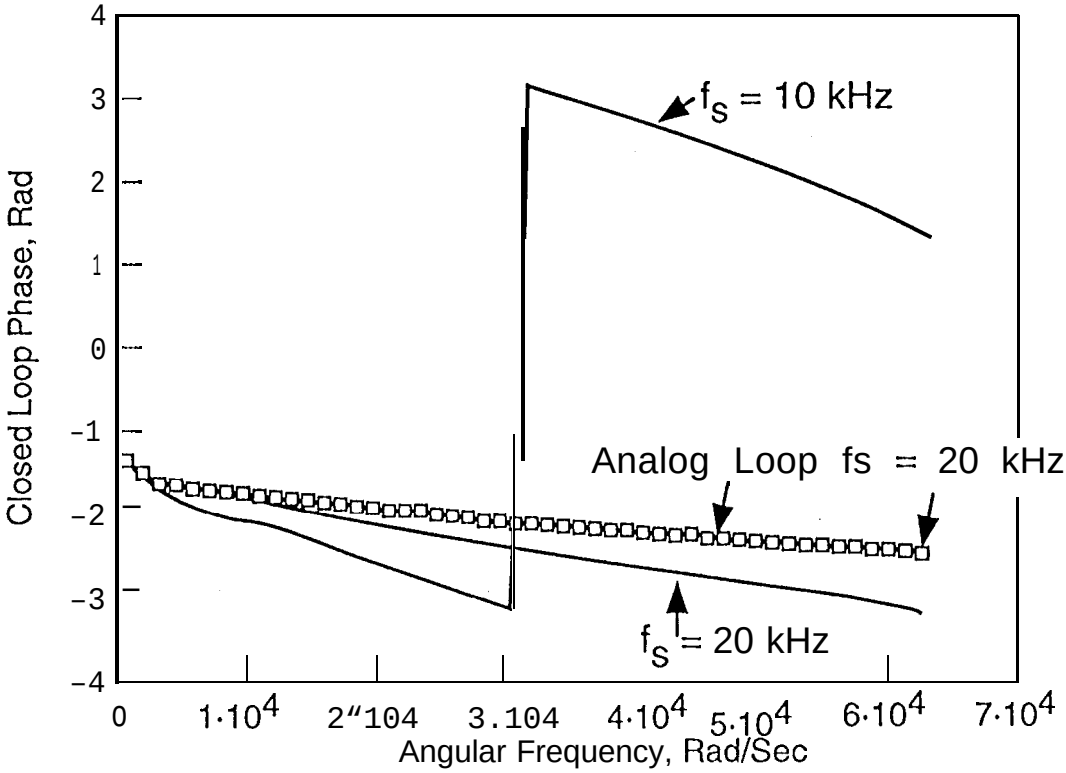

a. Plot of the Closed Loop Phase Characteristic

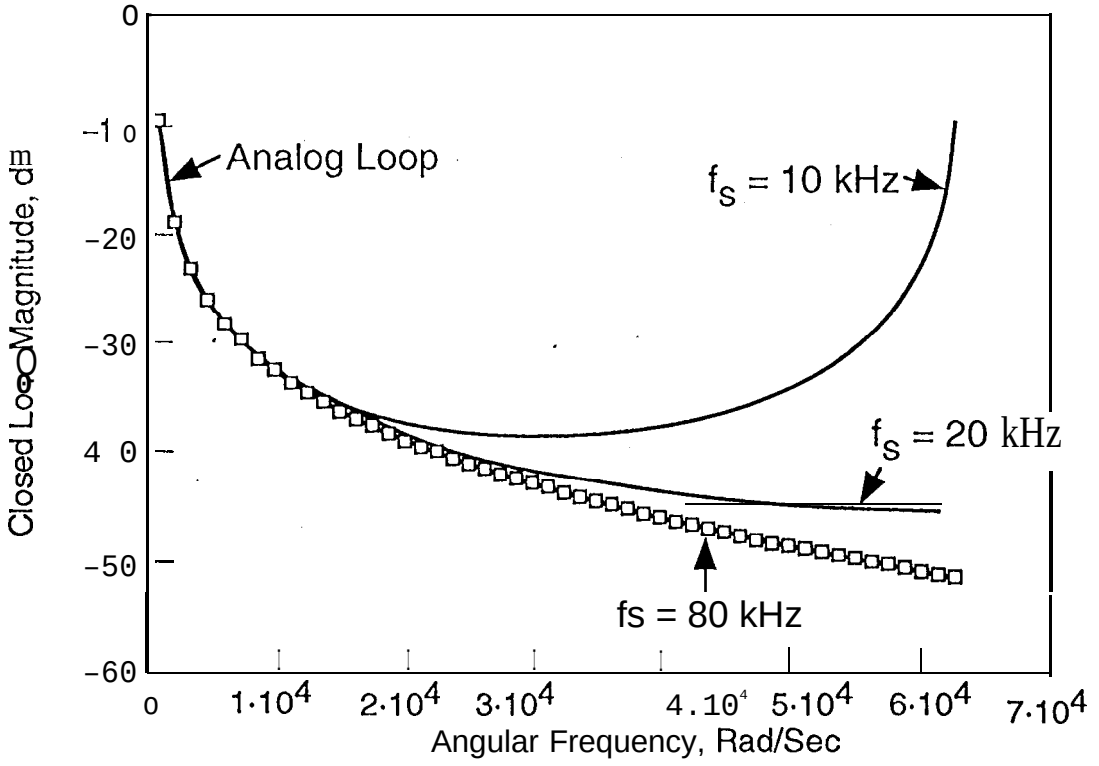

b. Plot of the Closed Loop Magnitude Response

Figure 7a. Recursive Implementation of the Open Loop Transfer Function $G_D(Z)$ Using Impulse Invariant Transformation Method

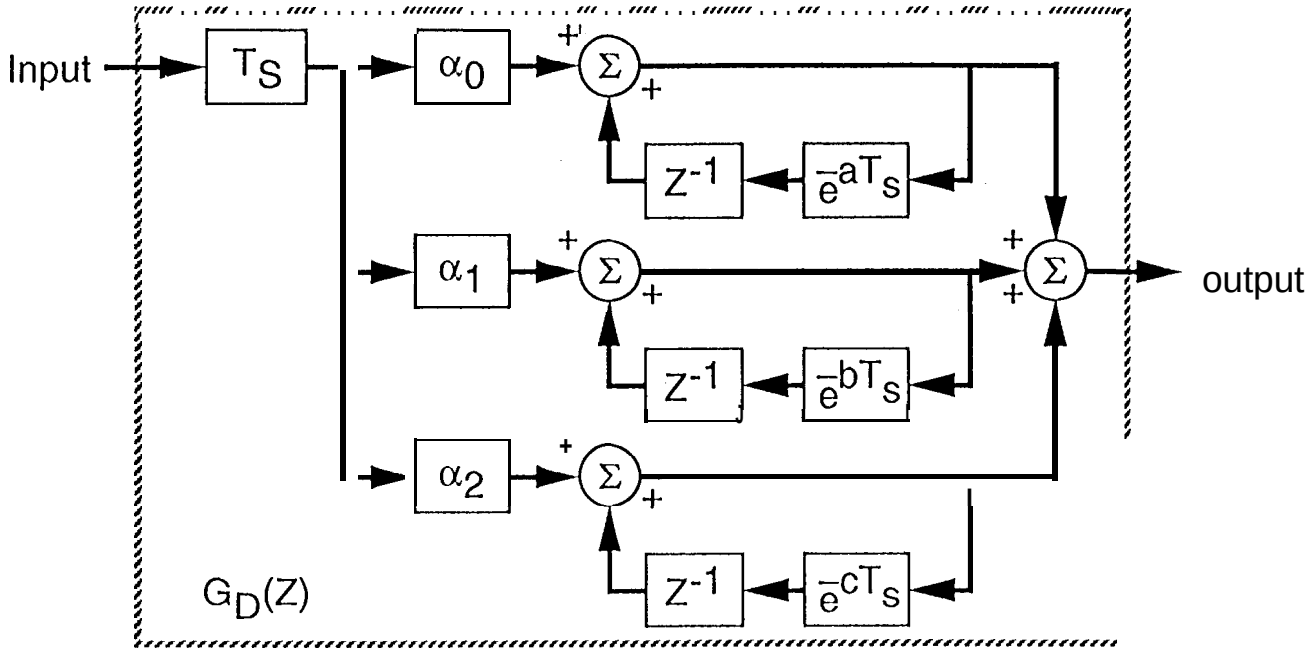

Figure 7b. Recursive Implementation of the Integrator K(Z) Using Impulse Invariant Transformation Method

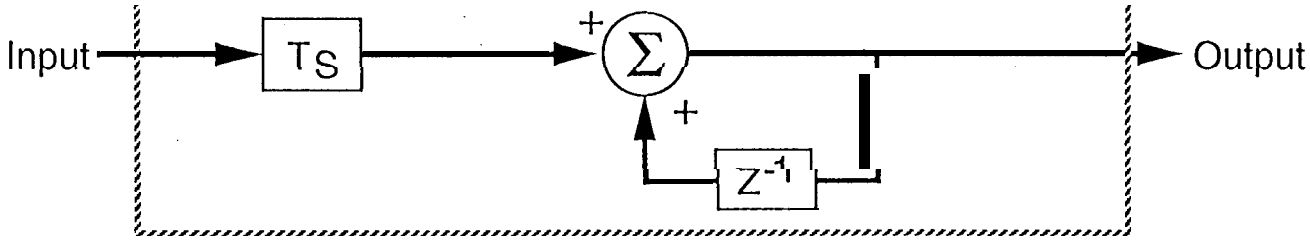

Figure 8. Closed-loop Response of the Digital Approximation Using Step Invariant Transformation Method

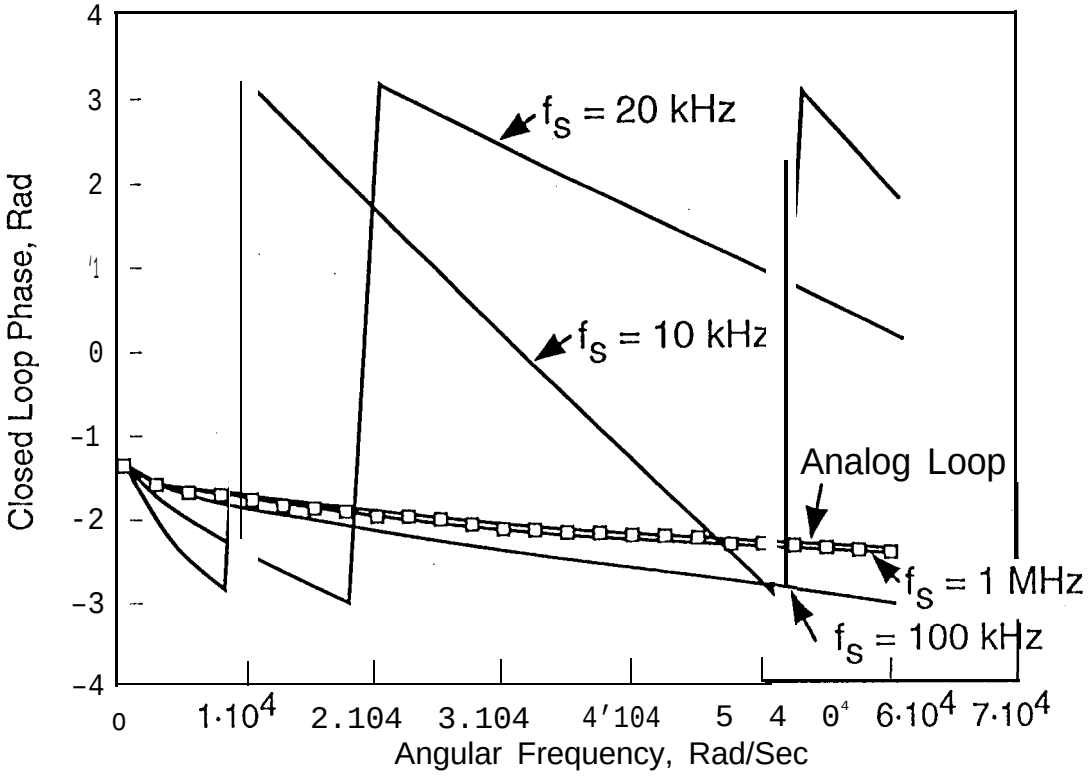

a. Plot of the Closed Loop Phase Characteristic

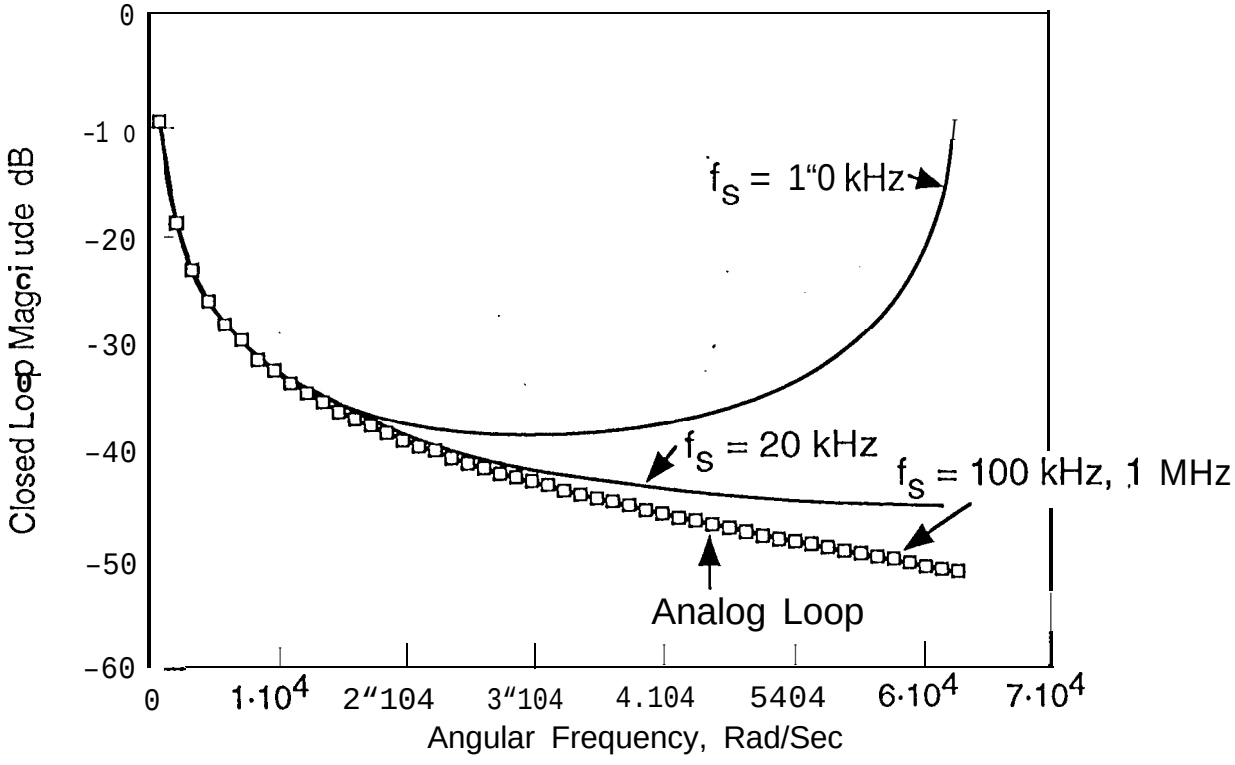

b. Plot of the Closed Loop Magnitude Response

Figure 9a. Recursive Implementation of the Open Loop Transfer Function $G_D(Z)$ Using Step Invariant Transformation Method

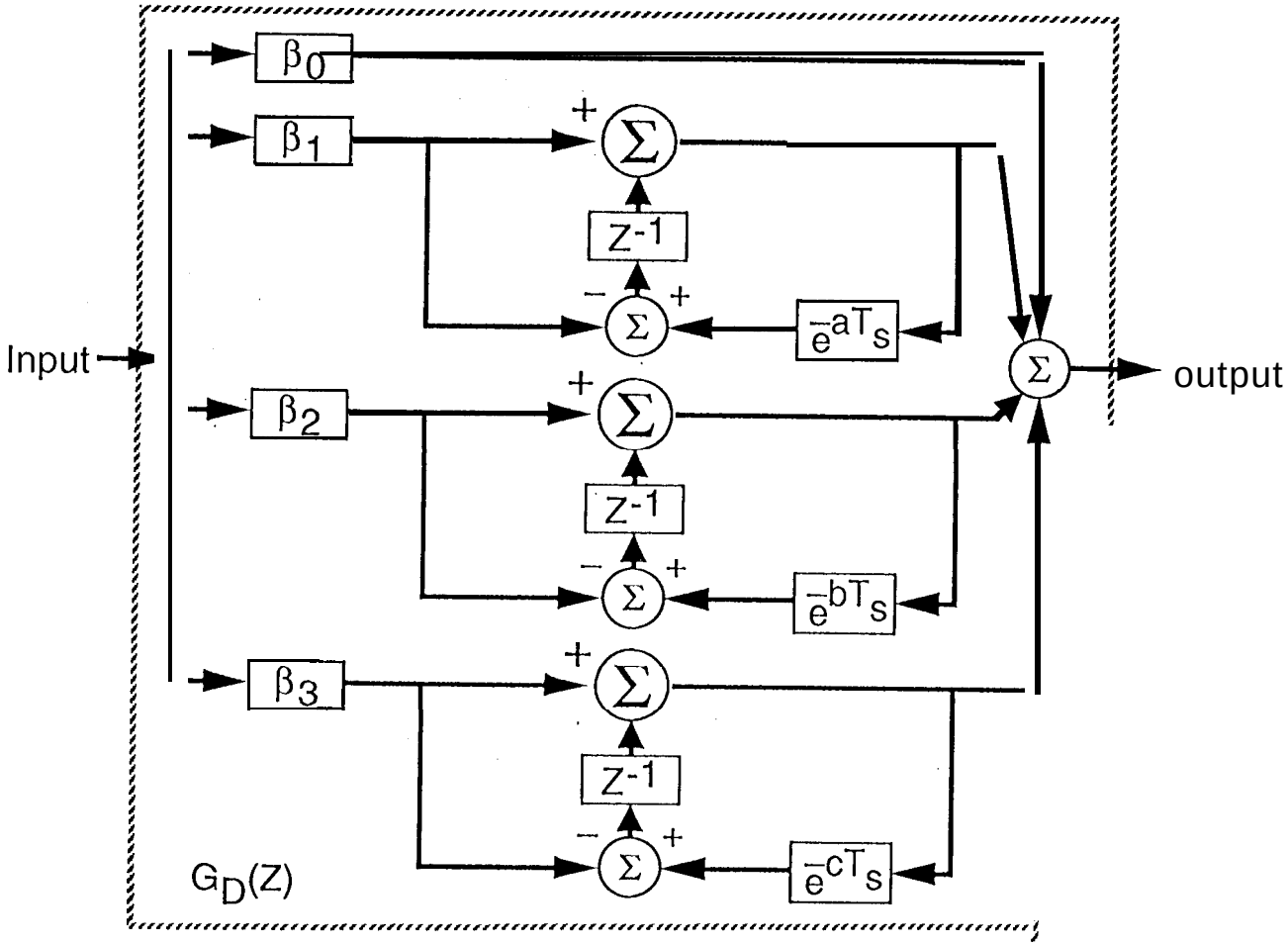

Figure 9b. Recursive Implementation of the Integrator K(Z) Using Step Invariant Transformation Method

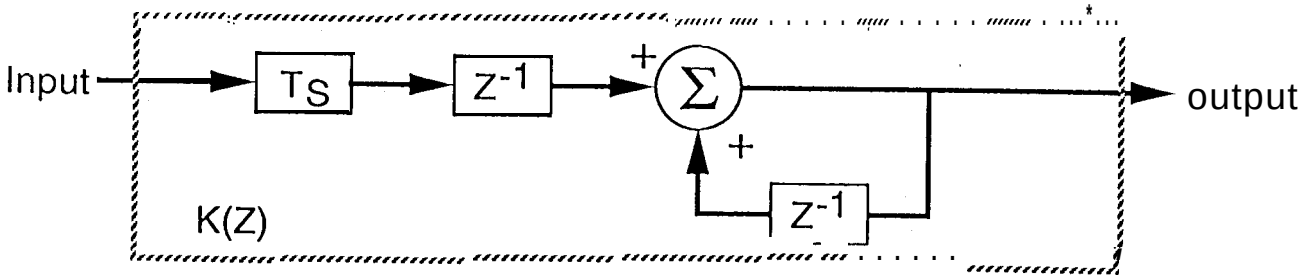

Figure 10. One-Sided Digital Loop Bandwidth

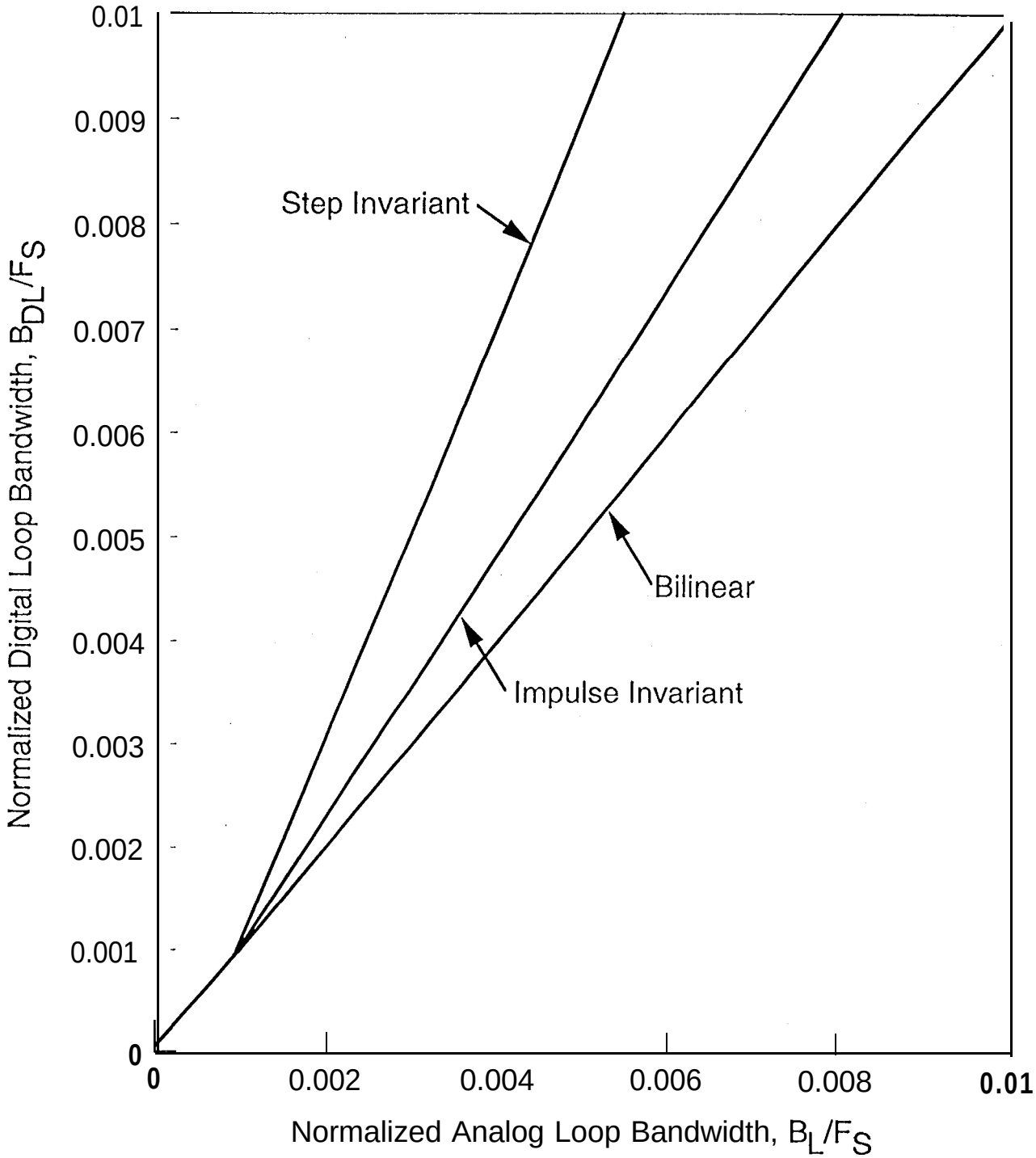

Figure 11. Theoretical Comparison of Tracking Jitter for Command-On

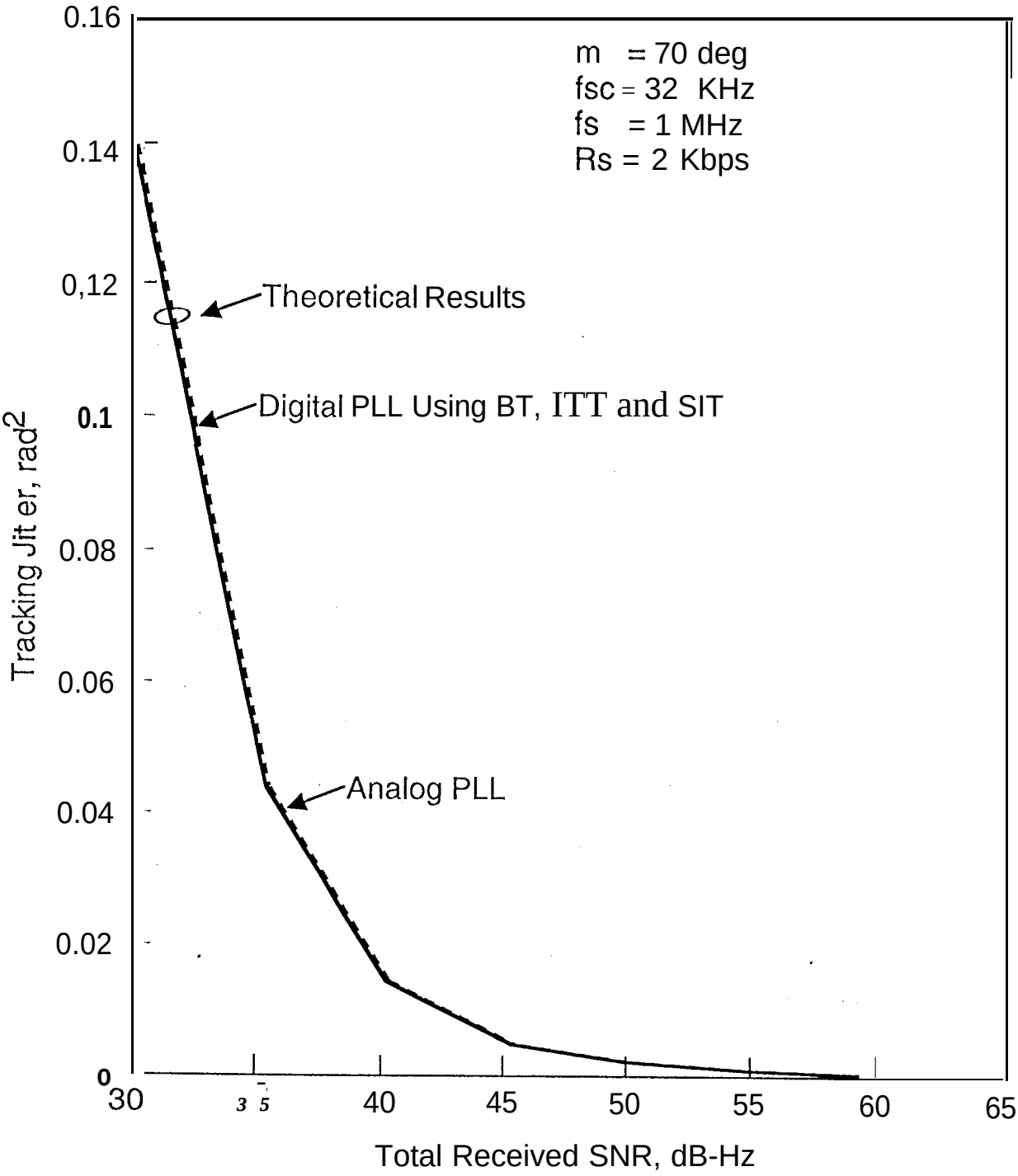

Figure 12. Tracking Phase Jitter Using Bilinear Transform

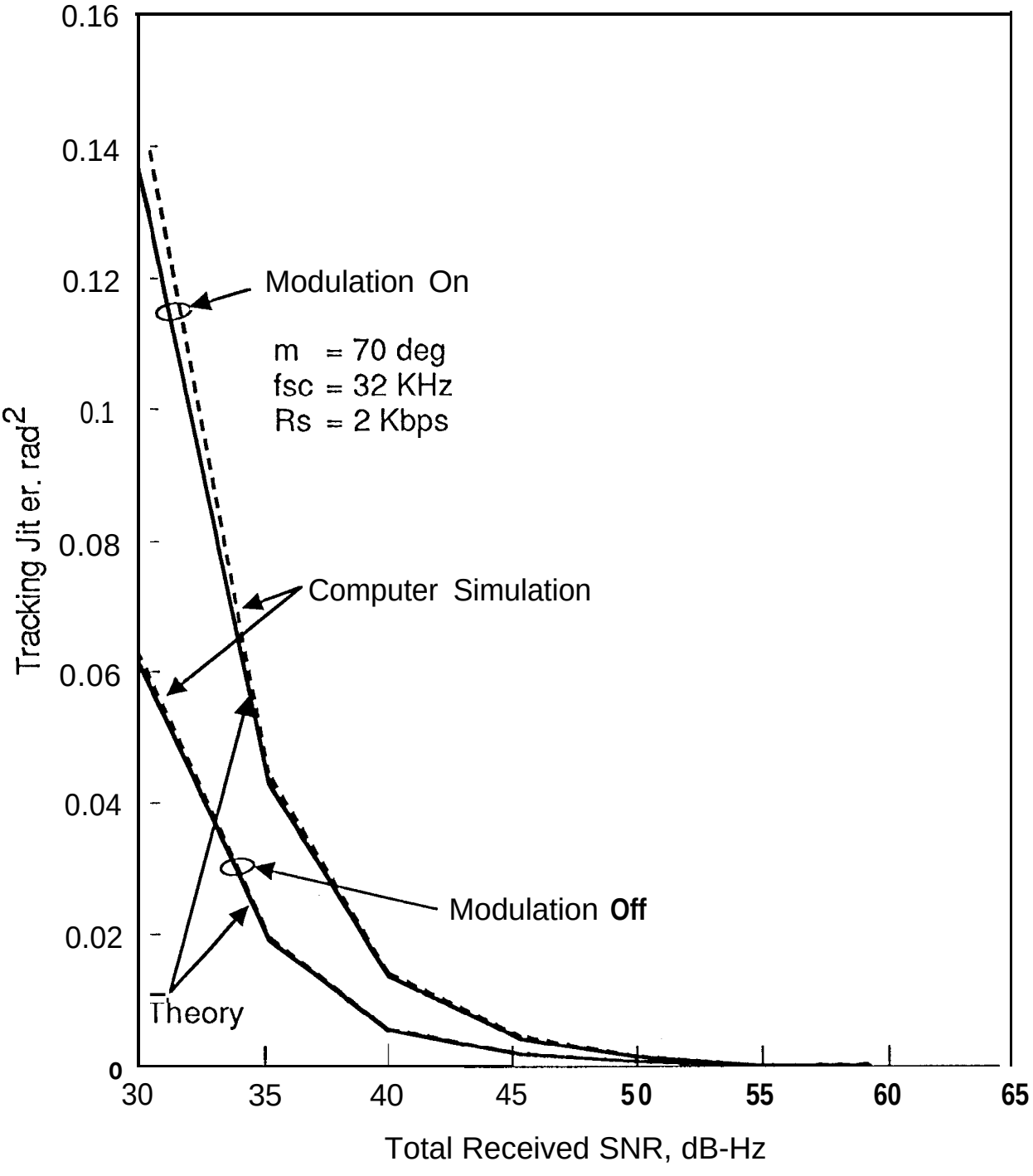

Figure 13. Carrier Loop SNR-vs-Total Received SNR

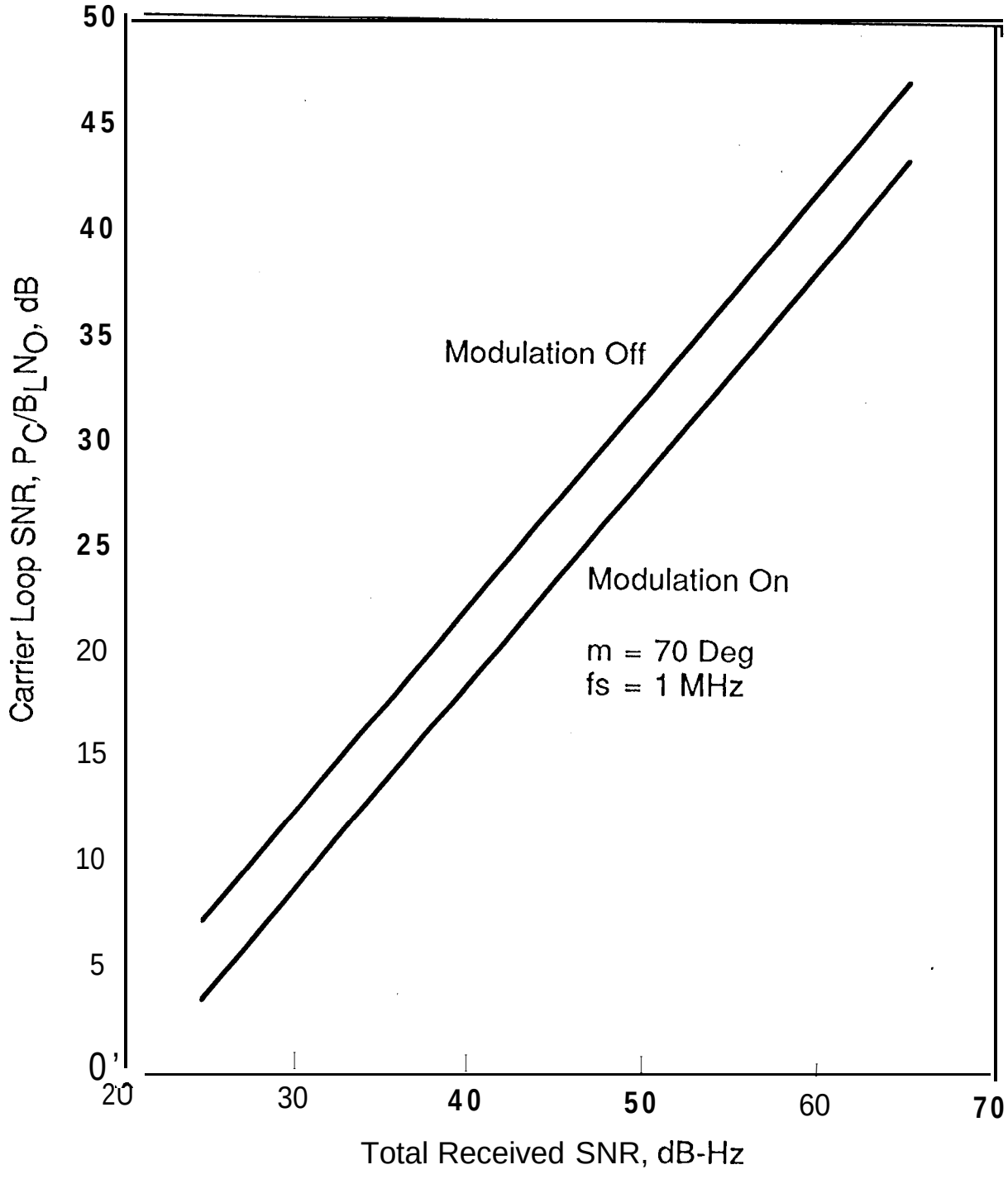

Figure 14. Comparison of the Tracking Phase Jitter